ACS NANO

Subscriber access provided by Argonne Research Library

Article

Crude-Oil-Repellent Membranes by Atomic Layer Deposition: Oxide Interface Engineering

Hao-Cheng Yang, Yunsong Xie, Henry Chan, Badri Narayanan, Lin Chen, Ruben Z Waldman, Subramanian K.R.S. Sankaranarayanan, Jeffrey W. Elam, and Seth B Darling

ACS Nano, **Just Accepted Manuscript** • DOI: 10.1021/acsnano.8b04632 • Publication Date (Web): 14 Aug 2018

Downloaded from http://pubs.acs.org on August 15, 2018

Just Accepted

"Just Accepted" manuscripts have been peer-reviewed and accepted for publication. They are posted online prior to technical editing, formatting for publication and author proofing. The American Chemical Society provides "Just Accepted" as a service to the research community to expedite the dissemination of scientific material as soon as possible after acceptance. "Just Accepted" manuscripts appear in full in PDF format accompanied by an HTML abstract. "Just Accepted" manuscripts have been fully peer reviewed, but should not be considered the official version of record. They are citable by the Digital Object Identifier (DOI®). "Just Accepted" is an optional service offered to authors. Therefore, the "Just Accepted" Web site may not include all articles that will be published in the journal. After a manuscript is technically edited and formatted, it will be removed from the "Just Accepted" Web site and published as an ASAP article. Note that technical editing may introduce minor changes to the manuscript text and/or graphics which could affect content, and all legal disclaimers and ethical guidelines that apply to the journal pertain. ACS cannot be held responsible for errors or consequences arising from the use of information contained in these "Just Accepted" manuscripts.

ACS Publications

is published by the American Chemical Society. 1155 Sixteenth Street N.W., Washington, DC 20036

Published by American Chemical Society. Copyright © American Chemical Society. However, no copyright claim is made to original U.S. Government works, or works produced by employees of any Commonwealth realm Crown government in the course of their duties.

Crude-Oil-Repellent Membranes by Atomic Layer Deposition: Oxide Interface Engineering

Hao-Cheng Yang[1], Yunsong Xie[2], Henry Chan[1], Badri Narayanan[1], Lin Chen[2], Ruben Z. Waldman[3], Subramanian K. R. S. Sankaranarayanan[1,4], Jeffery W. Elam[2,4], and Seth B. Darling[1,3,4]*

[1] Center for Nanoscale Materials, Argonne National Laboratory, Lemont, IL, 60439, USA

[2] Applied Materials Division, Argonne National Laboratory, Lemont, IL, 60439, USA

[3] Institute for Molecular Engineering, University of Chicago, Chicago, IL, 60637, USA

[4] Institute for Molecular Engineering, Argonne National Laboratory, Lemont, IL, 60439, USA

KEYWORDS anti-crude-oil, membrane, atomic layer deposition, oxides, hydration layer

ABSTRACT Crude oil fouling on membrane surfaces is a persistent, crippling challenge in oil spill remediation and oilfield wastewater treatment. In this research, we present how a nano-sized oxide coating can profoundly affect the anti-crude-oil property of membrane materials. Select oxide coatings with a thickness of ~10 nm are deposited conformally on common polymer membrane surfaces by atomic layer deposition to significantly mitigate fouling during filtration processes. TiO_2- and SnO_2-coated membranes exhibited far greater anti-crude-oil performance

than ZnO- and Al_2O_3-coated ones. Tightly bound hydration layers play a crucial role in protecting the surface from crude oil adhesion, as revealed by molecular dynamics simulations. This work provides a facile strategy to fabricate crude-oil-resistant membranes with negligible impact on membrane structure, and also demonstrates that—contrary to common belief—excellent crude oil resistance can be achieved easily without implementation of sophisticated, hierarchical structures.

Oily wastewater originating from oil spill accidents and industrial waste disposal poses a significant hazard to the environment and human health. Membrane technology receives burgeoning interest in oily wastewater treatment due to its high separation efficiency and low energy consumption.[1,2] Membranes have been widely implemented in oilfield wastewater treatment to meet reinjection or discharge standards. A major challenge, however, lies in mitigating severe membrane fouling by crude oil, which causes a dramatic decline of membrane performance and lifetime. The high viscosity and complex composition make crude oil extremely sticky to most of the membrane materials. Therefore, there is unmet demand for crude-oil-repellent membranes in the oil and gas industry, among others, despite some efforts to reduce oil fouling by stabilizing crude oil droplets with Pickering emulsion.[3]

Oil adhesion on a surface is closely related to the surface properties, and an ideal anti-oil surface would be hierarchically structured and fully hydrated. Water trapped in micro- and nano-structures reduces the contact area between oil and solid, and the hydration layer on the solid surface serves as a physical barrier to prevent direct oil adhesion.[4] Based on these design principles, many superhydrophilic/underwater-superoleophobic polymer membranes have been

developed for oil/water separation.[5–9] In general, these previously reported membranes are satisfactory for nonpolar solvents or light oils such as gasoline and diesel fuel, but unfortunately, few if any can resist crude oil. This failure is largely rooted in the lack of a stable, adequate, and robust hydration layer, in particular for surfaces composed of flexible polymer chains and the concomitant soft surface morphology. Hydrocarbon segments comprising the polymers are oleophilic, so they tend to reorient toward oil at the oil/water interface,[10] and water that may be initially trapped in a soft, rough structure is easily excluded under filtration pressure.[11] Therefore, non-flexible hydrophilic moieties and rigid roughness are favored in constructing a robust and stable anti-oil surface. For example, nanocellulose exhibits superior anti-oil performance relative to polyelectrolytes due to its abundant hydroxyl groups secured to a rigid molecular structure.[10] Zwitterionic polymers with high grafting density and tailored orientation can also achieve excellent anti-oil property due to the highly hydrated surface and limited flexibility.[12]

Inorganic minerals, such as calcium carbonate in clamshell,[13] are another category of material with rigid rough structure and plenty of hydrophilic moieties on the surface. Such structures can stabilize superoleophobicity even under filtration pressure and cross flow. For instance, Liu *et al*. fabricated a hierarchical CuO surface with excellent underwater superoleophobicity by mimicking the surface structure of clamshell.[13] Another work by Guo *et al*. presented a nacre-inspired composite surface composed of montmorillonite and hydroxyethyl cellulose with extremely low oil adhesion.[14] Similarly, oil/water separators could be fabricated by growing inorganics such as copper oxide nanowires,[15] cupric phosphate nanosheets[16] and zeolites[17] on steel meshes. Most of them, however, are only realizable on large-pore materials such as meshes, fabrics, and sponges rather than membranes, because using those synthetic methods, minerals aggregate into micron-sized particles (*i.e.* larger than membrane pores). These separation

materials cannot meet the requirements of oilfield wastewater treatment because of their poor rejection of sub-micron contaminants.[18] In addition, the poor compatibility between inorganics and polymers renders realization of conformal and stable mineral coatings on polymer substrates an ongoing challenge. Xu's group developed a bio-inspired mineralization strategy to fabricate conformal mineral nano-coatings on polymer microfiltration membranes.[11,19–21] A polyacrylic acid or polydopamine/polyethyleneimine interlayer was introduced on the membrane surface for in-situ mineral growth. The interlayer not only promotes the uniformity and stability of mineral coatings, but also stabilizes their amorphous structure to confine their thickness within several tens of nanometers. Unfortunately, the coating thickness is poorly controlled, and only a few minerals are available by this strategy.

Atomic layer deposition (ALD), in contrast, provides a reliable technology to fabricate conformal coatings on material surfaces. The coating thickness can be precisely tuned at the nanometer scale by adjusting deposition parameters. Some researchers have applied this technology to modify polymer membranes for various applications.[22–27] Although several research groups have reported the application of ALD (or related methods) for material surface modification (*e.g.* sponge, fabric) for oil/water separation, the ALD layer served as an initial layer for post-modification in these instances.[28–31] Herein, we fabricated a series of oxide-coated membranes by ALD and evaluated their anti-crude-oil performance. Oxides from different element groups (*i.e.* ZnO, Al_2O_3, TiO_2 and SnO_2) exhibited vastly different crude oil repellence: ZnO- and Al_2O_3-coated membranes remained as adhesive to crude oil as nascent membranes, while TiO_2- and SnO_2-coated ones exhibited extraordinary low adhesion to crude oil both under water and in air after wetting by water. The underlying mechanism, revealed by molecular

dynamics (MD) simulations, is much tighter hydration layers on the surfaces of SnO_2 and TiO_2, which protect them from the adhesion of crude oil.

RESULTS AND DISCUSSION

Commercial polyvinylidene fluoride (PVDF) membranes were selected as the substrate in our research because the polyvinyl pyrrolidone (PVP) embedded as a hydrophilic additive introduces nucleating sites for the ALD process, which would otherwise be challenging on a largely unreactive PVDF substrate. Such hydrophilic polymer membranes are widely used in industrial separations, rendering this material a proper reference in our anti-oil testing. Considering the low thermal stability of polymer membranes, the ALD temperature for all samples was 100 °C, much lower than the melting point of PVDF (~170 °C). For this reason, only oxides that could form at low temperature with suitable precursors were selected (*i.e.* ZnO, Al_2O_3, TiO_2 and SnO_2, **Table S1** in Supporting Information). It should be mentioned that the selection of ALD precursors may influence the surface wettability of the ALD coatings, because by-products of interfacial reactions may participate in the formation of chemical bonds.[28] The number of ALD cycles was selected to achieve a comparable thickness (*i.e.* ~10 nm) for each of the different oxide coatings (**Table S2**).

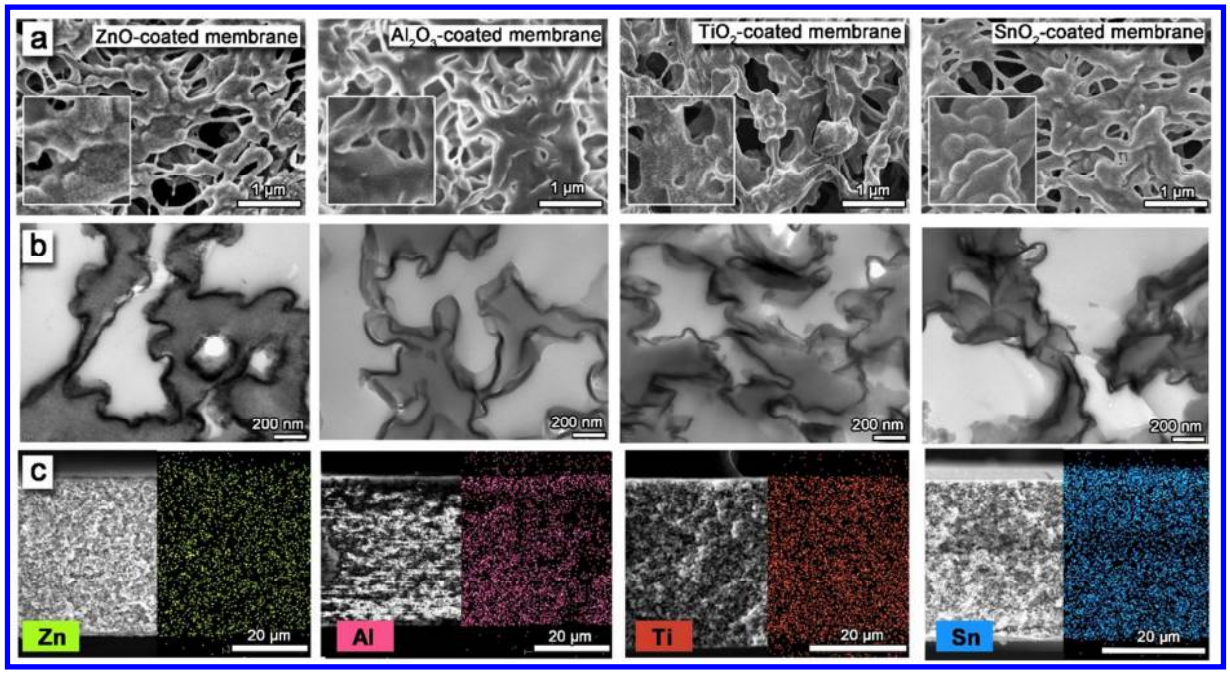

Figure 1. a) FE-SEM and b) TEM images of membranes coated with ZnO, Al_2O_3, TiO_2, and SnO_2. c) EDS images of membrane cross-sections.

Surface morphology has a significant impact on surface wettability according to the Cassie-Baxter and Wenzel models.[32,33] We observed the surface structure of nascent and oxide-coated membranes by field emission scanning electron microscopy (FE-SEM) as shown in **Figure 1a**. The initial PVDF membrane is a commercial product fabricated by phase inversion. These membranes have an irregular and bicontinuous porous structure with smooth solid surfaces (**Figure S1** in Supporting Information). As mentioned above, PVP was embedded in the membrane as a hydrophilic additive, and its polar moieties could interact with vapor-phase precursors for nucleation during ALD. Compared with the nascent membranes, the Al_2O_3- and SnO_2-coated membranes show no obvious changes in surface morphology, while a slight increase in surface roughness can be observed on TiO_2- and ZnO-coated membranes, attributed to the different nucleation processes on the membrane surface. All of the coated membranes appeared granular at high resolution (**Figure 1a**, insets) suggesting a roughened surface, but this

effect was most noticeable for the ZnO-coated membrane. Surface roughness can result from a nanocrystalline ALD film or from slow nucleation on the PVP surface that leads to 3D island growth and coalescence. We expect all of the ALD films to display inhibited growth due to the absence of hydroxyl groups on the PVP surface. The ZnO coating shows the highest roughness, and this is likely because it is crystalline while other oxides are all amorphous (**Figure S2** in Supporting Information). If solely considering the surface structure, ZnO and TiO_2 would be expected to have superior anti-oil property because the micro-nano composite structure could minimize the direct contact area between oil and membrane and promote surface oleophobicity under water. The TEM images of the membrane slices demonstrate that a uniform and conformal coating formed on membrane surface for all the oxides (**Figure 1b**), and the EDS spectra of membrane cross-sections also indicate a uniform distribution of oxide across the entire membrane (**Figure 1c** and **S3**).

To evaluate the surface wettability of the membranes, we measured the water contact angles (WCAs) and underwater oil contact angles (OCAs) on each membrane surface. Because of the PVP additive, the nascent membranes are moderately hydrophilic and a water drop can gradually penetrate through due to the capillary effect of the porous structure (**Figure 2a**). The membrane surface became substantially more hydrophilic following ALD treatment. Water drops permeate through the membranes far more rapidly after coating with TiO_2 or SnO_2 **(Figure 2b)**. The hydrophilicity is closely related to the underwater oleophobicity. The underwater OCAs were detected by using crude oils with low and high viscosity (**Figure 2c**). All the membranes, including the nascent one, are oleophobic underwater because of their hydrophilicity (or high surface energy) in air. Crude oils are sticky to the nascent, ZnO-coated, and Al_2O_3-coated membranes. The nascent membrane shows an OCA of 124.8 ± 3.5°, and the ZnO- and Al_2O_3-

coated membranes perform similarly or even less oleophobic (OCAs of 104.4 ± 3.4° and 123.5 ± 2.2°, respectively). In contrast, both TiO_2- and SnO_2-coated membranes show an OCA above 160°, indicating the superoleophobicity of their surfaces. To separate the influences of membrane structure on OCAs, we also measured the underwater OCAs on silicon wafers coated with the same oxides (**Figure 2d**). The underwater OCAs on flat surfaces decrease significantly, and follow the order: SnO_2>TiO_2>Al_2O_3>ZnO. Specifically, the OCA on ZnO decreases to 54.9 ± 2.7°, lying in the oleophilic region, while the TiO_2 and SnO_2 surfaces remain oleophobic with OCA values of 115.8 ± 4.3° and 119.2 ± 6.9°, respectively.

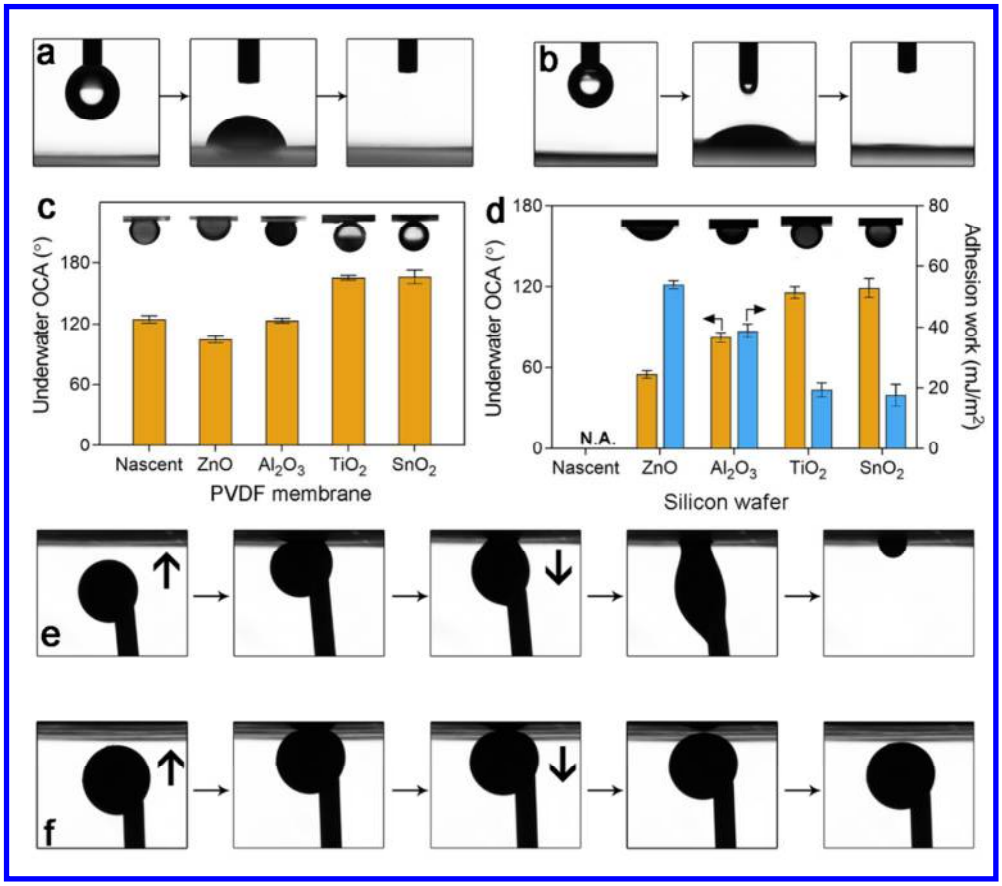

Figure 2. Water contact angles on a) nascent and b) SnO_2-coated membranes (water droplets permeated through other oxide-coated membranes similarly). c) Crude oil contact angles (OCAs)

on nascent and oxide-coated PVDF membranes under water. d) OCAs on oxide-coated silicon wafers under water. Crude oil adhesion test on e) nascent and f) SnO_2-coated membranes.

Oil adhesion work on the surfaces under water is defined as the work needed to separate oil and surface in water, which can reflect the strength of adhesion between oil and substrates. We calculated the underwater adhesion work based on the following equation: $W=\gamma(1+cos\theta)$, in which γ is the interfacial tension between crude oil and water, and θ is the underwater OCA on the surface (**Figure 2d**, blue bars).[34] Adhesion work is closely related to the underwater OCA, that is, a larger OCA corresponds with lower adhesion work. The SnO_2 surface shows the lowest adhesion work of 17.64 ± 2.90 mJ/m^2 as expected. These results on smooth, planar silicon wafers indicate that the intrinsic hydrophilicity (or hydration state) of oxides represents a larger contribution to the surface oleophobicity underwater relative to surface roughness. In another experiment, we applied an extremely sticky crude oil for a dynamic adhesion test. The crude oil is exceedingly sticky to the nascent PVDF membrane (**Figure 2e**). In contrast, no adhesion or deformation was observed when the oil droplet was pushed toward or pulled away from the SnO_2-coated membrane in water (**Figure 2f**).

Wetting and adhesion of crude oil on a surface are closely related to the surrounding environment. A hydrophilic surface always shows oleophobicity in water but oleophilicity in air. Therefore, we investigated the crude oil adhesion on membrane surfaces both under water and in air. In the first experiment, the membranes were fouled by high-viscosity crude oil in air and then immersed in water (**Figure 3a**). Membranes were prewetted by water before contacting crude oil, because the anti-oil property arises from the hydration layer. Crude oil stayed on nascent and ZnO-coated membranes without obvious change after immersing in water, while it departed readily from the surface in the case of TiO_2- and SnO_2-coated membranes. For the Al_2O_3-coated

membrane, crude oil deformed to a sphere with a large OCA but remained on the membrane surface. This is a result of the balance among buoyancy, surface tension, and adhesion force in an aqueous environment. A speculated mechanism is depicted in **Figure 3b**. In the case of the nascent and ZnO-coated membranes, the hydration layer is unstable, which therefore cannot prevent contact between the crude oil and the membrane surface in air. Upon immersing in water, water molecules cannot insert themselves between the adhered crude oil and the membrane surface. On the other hand, the hydration layer is tightly bonded on the TiO_2 and SnO_2 surfaces, which forbids direct contact between oil and surface, and crude oil easily detaches from the surface due to the ultra-low adhesion and floats on the water because of its buoyancy. For the Al_2O_3-coated membrane, the surface is partially hydrated when contacting crude oil, resulting in moderate oil adhesion and a relatively high OCA balanced by buoyancy and surface tension (**Figure S6**). To exclude buoyancy itself as a major reason underlying the anti-oil property, we conducted another experiment to rinse the crude-oil-fouled membrane with water in the air instead of immersing them in water. As shown in **Figure 3a**, crude oil on the TiO_2 and SnO_2-coated membranes were easily washed off whereas it remained on the nascent, ZnO-coated, and Al_2O_3-coated membranes. Stability of anti-oil properties during long-term storage is another important issue for these membranes. Surfaces modified by hydrophilic polymers always suffer from hydrophobicity recovery during storage due to chain rearrangement to minimize the surface energy in the air. In contrast, oxide-coated membranes show stable superoleophobicity after long-term (three-month) storage in the air because of their rigid hydrophilic groups.

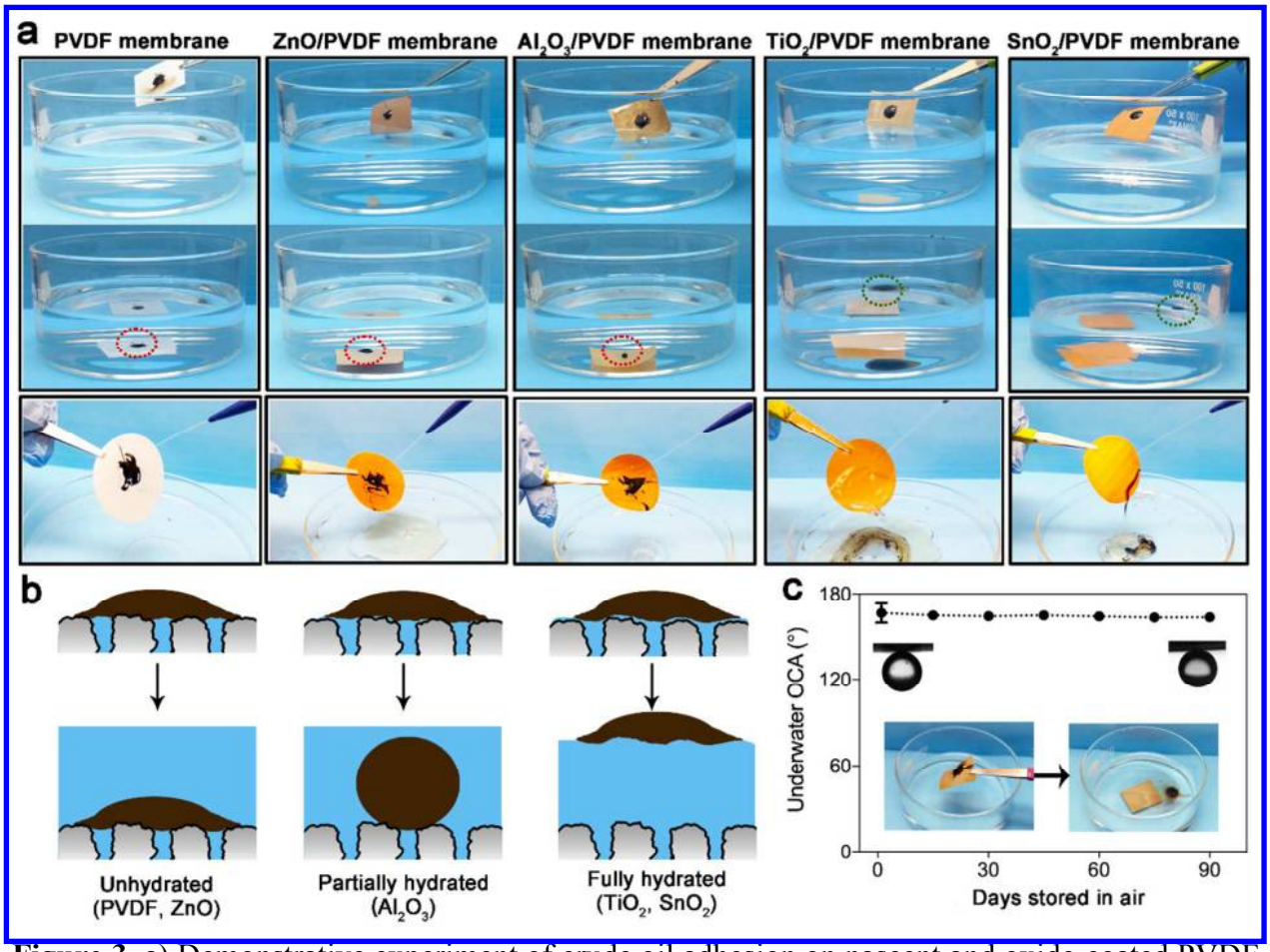

Figure 3. a) Demonstrative experiment of crude oil adhesion on nascent and oxide-coated PVDF membranes. b) Speculated mechanisms for crude oil adhesion on, or departure from, the membrane surfaces. c) Underwater OCAs on SnO_2-coated membranes after long-term storage in air. The inserts are the crude oil contact angle and crude oil adhesion on SnO_2 membrane after stored in air for 90 days.

The anti-oil performance for these oxides is a consequence of their hydration states, *i.e.*, the interactions between the various oxides and water. We employed classical molecular dynamics (MD) simulations (See Methods for details) to investigate the oxide-water interactions at the atomic scale. Both pristine and hydroxylated slabs of amorphous Al_2O_3, TiO_2, and SnO_2 were studied (**Figure 4a**). (ZnO was not included in these simulations because of the lack of a suitable

interatomic potential.) These simulations show that the wettability of the surfaces is strongly governed by the nature of the oxide, in increasing order Al_2O_3 (least) < TiO_2 < SnO_2 (highest). The water-surface interactions are characterized by analyzing the radial distribution functions (RDFs) of oxygen of water with the surface cation (Sn, Ti, and Al, respectively). Regardless of the oxide, these RDFs show two distinct peaks associated with the first and second solvation layers of water near the interface (**Figure 4b**). Water adsorbs layer-by-layer with a relatively weak cohesion between the adjacent layers. The first layer of water adheres strongly to the surface (as indicated by the sharp first peak in the RDF), while the second layer is weakly attached to the surface resulting in a relatively broad second peak. The dynamic relaxation in the interfacial layer can extend to microseconds and up to hundreds of picoseconds in the next proximal layer. Note that the separation distance between the surface and the first layer of water shown by the position of the first RDF peak, as well as the peak intensities, are strongly dictated by the nature of the oxide. For SnO_2 and TiO_2, the proximal water layer is much closer to the surface (SnO_2: 1.5 Å; TiO_2: 1.8 Å) as compared to Al_2O_3 (2.6 Å); this, along with the higher peak intensities, suggests strong interactions between water and SnO_2 or TiO_2 (SnO_2-water being stronger). On the other hand, lower peak intensities in the Al_2O_3-water RDF suggest a relatively weak interaction with water molecules.

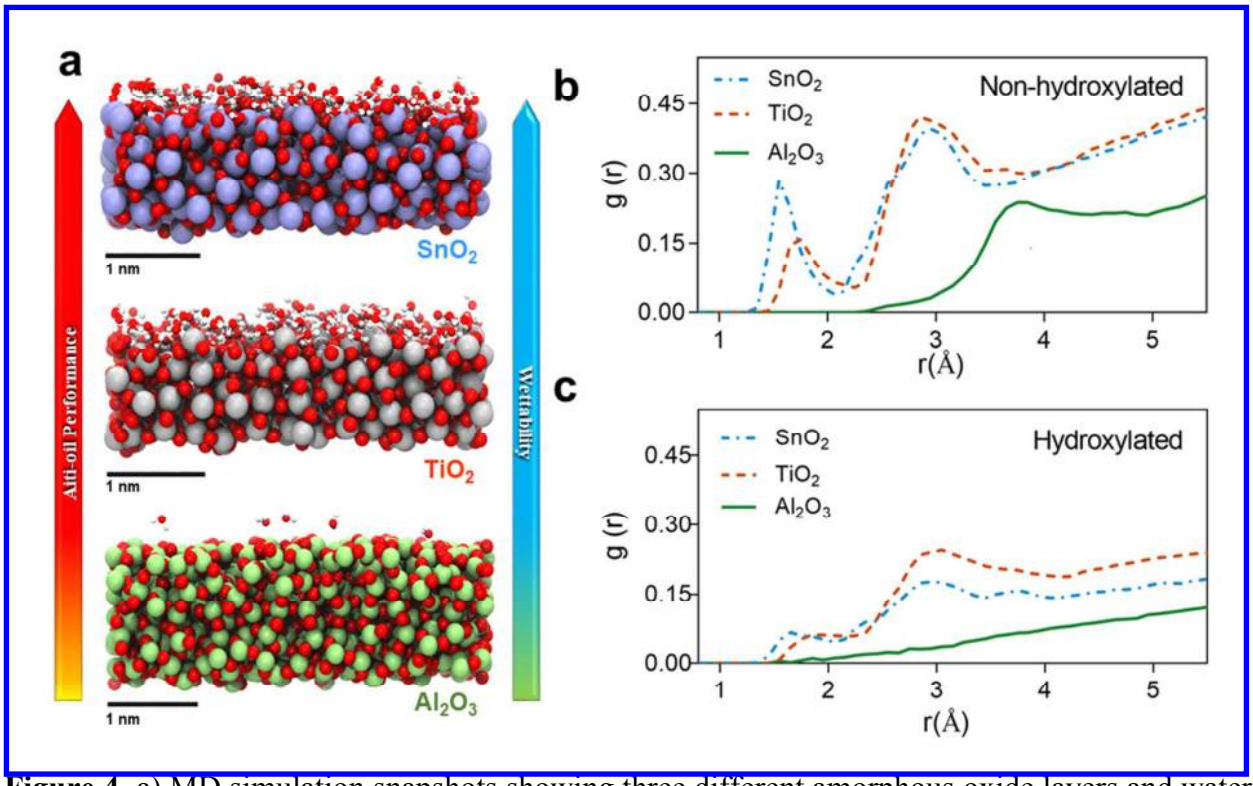

Figure 4. a) MD simulation snapshots showing three different amorphous oxide layers and water molecules that are within 3.4 Å above their surfaces. The atoms are colored by their types, *i.e.*, O (red), H (white), Sn (purple), Ti (grey), Al (green). From bottom to top, the wettability of these amorphous oxide layers increases, which is characterized by the water-oxide radial distribution functions, g(r), shown in b) for non-hydroxylated (pristine) and in c) for hydroxylated oxide layers.

Analysis of the structure of water near the oxide surfaces reveals the formation of more-ordered structures for SnO_2 (number of neighbors per water, Z~4.95) and TiO_2 (Z~4.6) as opposed to Al_2O_3 (Z~1). The hydroxylated surfaces also follow the same trend in wettability *i.e.* the order of affinity to water is Al_2O_3<TiO_2<SnO_2 (**Figure 4c)**. Note, the larger lattice parameters of SnO_2 (compared to other oxides) leave more space between terminal and bridging hydroxyls, which

allows the second layer molecules to come closer to the surface. Formation of a stronger and more well-ordered water structure near an oxide surface is expected to sterically hinder the interaction of oil with the surface, and consequently provide better anti-crude-oil performance. Thus, based on the extent of water-ordering assessed by MD simulations, the increasing order of anti-oil performance is predicted to be Al_2O_3<TiO_2<SnO_2, consistent with our experiments described above (**Figures 2** and **3**).

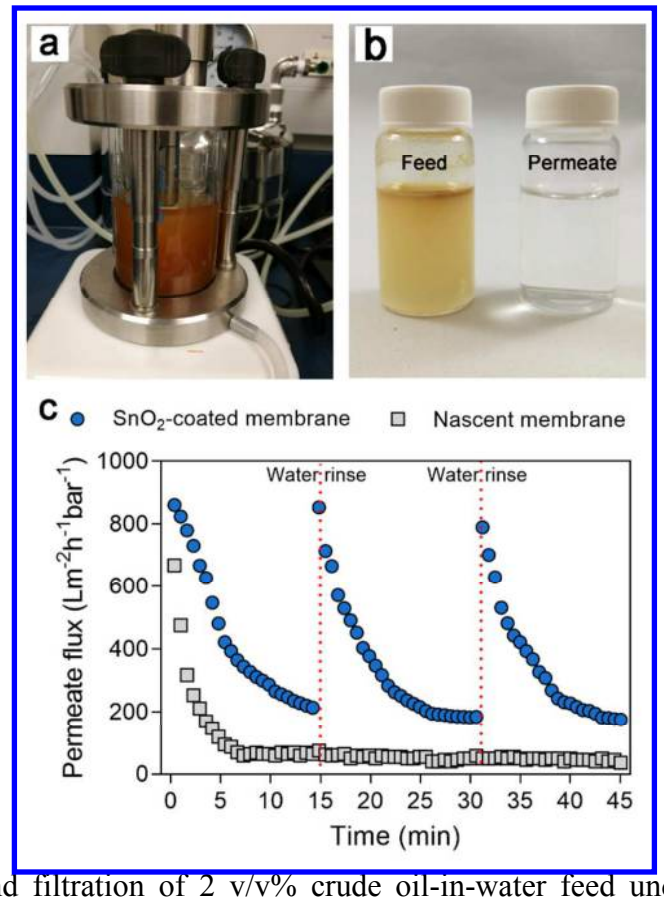

Figure 5. a) Dead-end filtration of 2 v/v% crude oil-in-water feed under stirring. b) Digital pictures of the feed and permeate. c) Permeate flux evolution of nascent PVDF and SnO_2-coated membranes.

Because of its excellent anti-oil properties, SnO_2-coated membranes were applied in realistic oily wastewater filtration experiments. Flux evolution over time will reflect the degree of fouling

on the membrane surface. For comparison, we also measured the flux of nascent membranes (**Figure 5**). The concentration of crude oil in water is 2 v/v%, and vigorous stirring was applied to simulate the dynamic filtration process. Both types of membranes exhibited similar initial flux of ~800 $Lm^{-2}h^{-1}bar^{-1}$. The permeate flux of the nascent membrane, however, decreased sharply to ~50 $Lm^{-2}h^{-1}bar^{-1}$ due to severe membrane fouling. Moreover, oil eventually passed through the membrane because of the severe fouling in the membrane pores (**Figure S7** in Supporting Information). In contrast, the SnO_2-coated membrane showed slower and less pronounced decrease in permeate flux, and even this moderate decrease is likely attributable to pore blocking during dead-filtration rather than fouling per se. Moreover, no flux recovery was observed for the nascent membrane, while the flux was nearly completely recovered for the SnO_2-coated membrane after the first rinsing by water. The flux of the SnO_2-coated membrane shows some irreversible decrease after several cycles, but its flux was still much higher than that of the nascent one (~200 $Lm^{-2}h^{-1}bar^{-1}$), indicating substantial improvement in anti-crude-oil performance. Most of the oil droplets within the emulsion fall into the 400–700 nm size range (**Figure S8**), and the total carbon content is decreased from 2845 ppm to 82.26 ppm, corresponding to a rejection rate of 97.11%. The unrejected organics are the dissolvable components in crude oil.

CONCLUSION

In conclusion, we demonstrate an attractive strategy to fabricate crude-oil-repellent membranes by oxide surface engineering. ALD provides a simple, adaptable, and tunable means of modifying the interfacial properties of polymer membranes by imparting them with mechanically

rigid hydrophilicity. MD simulations revealed that the significant differences in crude oil resistance originated from the different hydration state of the various oxides. TiO_2 and SnO_2 surfaces display much higher water molecule densities near the surface and stronger interactions with water. Such tightly bound hydration layers protect these membranes from fouling by crude oil. The coatings are robust, stable over time, and offer demonstrated resistance to fouling under oil-in-water filtration. This research also indicated select oxides lacking sophisticated structures and complicated composition could achieve outstanding anti-crude-oil property, which inspires further research into high-performance membranes for the oil and gas industry.

MATERIALS AND METHODS

Atomic layer deposition (ALD): Poly(vinylidene fluoride) (PVDF) microfiltration membranes (ϕ 47 mm, mean pore size 200 nm) were purchased from MilliporeSigma (USA). The precursors, *i.e.* diethyl zinc (DEZ), trimethyl aluminum (TMA), titanium tetrachloride (TTC), and tetrakis(dimethylamino) tin(IV) (TDMASn) were obtained from Sigma-Aldrich (USA). All the chemicals were used as received. ALD was conducted in a hot-walled, viscous flow reactor constructed by a circular stainless-steel tube with an internal diameter of 5 cm.[35] All the experiments were performed at 100 °C using ultrahigh purity (99.999%) nitrogen carrier gas. The growth rates of the ALD oxides were measured using spectroscopic ellipsometry (alpha-SE, J. A. Woollam Co.) on films deposited on silicon (100) wafer coupons. A long dose (5 s) and purge time (40 s) was applied to allow the diffusion of precursors through the entire membrane.

Characterization: The surface morphologies of the membranes were characterized by field emission scanning electron microscopy (FE-SEM, Hitachi). The membrane slices were prepared by infiltrating epoxy resin into the membrane and sliced up after solidification, and then

observed under a transmission electron microscope (TEM, JEOL). The crystalline information was detected by an X-ray diffractometer (D2 Phaser, Bruker AXS). The surface hydrophilicity as well as the underwater oleophobicity was evaluated using a water contact angle test system (FM40, KRÜSS). To measure the underwater oil contact angles on the membranes, the samples were settled upside-down, and the oil was pumped from a bent needle. In the oil adhesion test, the membranes were pre-wetted by water for 1 min, and residual water on the membrane surface was adsorbed using filter paper. A ~50 μL oil droplet was deposited on the membrane surface, and the membrane was then re-immersed in the water. The oil/water separation test was performed with a dead-end filtration unit with an effective separation area of 13.8 cm^2 (EMD Millipore). Stirring was applied to mitigate fouling caused by cake layer formation. The feed was filtrated by the membrane perpendicularly, and the operating pressure was tuned by nitrogen gas. Crude oil with low viscosity was applied in this experiment, and the concentration was 2 v/v%.

Molecular Dynamics simulations: The wettability of various amorphous oxide surfaces is investigated in atomistic MD simulations performed using LAMMPS. Each system roughly consists of a 4 nm × 4 nm × 1.3 nm oxide slab with a block of SPC/E water placed 0.2 nm above its surface. The interactions between atoms within the oxide layers are modeled using the Buckingham potential, while their cross interactions with water are modeled using a combination of Lennard-Jones and Coulomb potentials. The force field parameters for pristine SnO_2, TiO_2, and Al_2O_3 oxide layers and their hydroxylated forms are based on previous reports respectively.[35–37] The oxide systems were equilibrated for at least 100 ps under an isothermal-isobaric ensemble at T=300 K and P=1 bar. Radial distribution functions were calculated from the last 1 ps of each simulation.

ASSOCIATED CONTENT

Supporting Information.

The following files are available free of charge.

Figures showing the XRD and EDX spectra of the oxide-coated membranes, TEM images of membrane slices, scheme of the oil contact angle test, photograph of oil-rejecting failure of the nascent membrane. Tables of ALD conditions and oxide coating thickness. (PDF)

Videos showing crude-oil-fouled membranes being immersed into a water bath, demonstrating that nascent, ZnO-coated, and Al_2O_3-coated membranes remain fouled, whereas TiO_2-coated and SnO_2-coated membranes release the oil immediately (.avi format).

AUTHOR INFORMATION

Corresponding Author

*E-mail: darling@anl.gov

ACKNOWLEDGMENT

Use of the Center for Nanoscale Materials, an Office of Science user facility, was supported by the U. S. Department of Energy, Office of Science, Office of Basic Energy Sciences, under Contract No. DE-AC02-06CH11357. This material is based upon work supported by Laboratory Directed Research and Development (LDRD) funding from Argonne National Laboratory, provided by the Director, Office of Science, of the U.S. Department of Energy under Contract No. DE-AC02-06CH11357.

REFERENCES

(1) Cheryan, M.; Rajagopalan, N. Membrane Processing of Oily Streams. Wastewater Treatment and Waste Reduction. *J. Memb. Sci.* **1998**, *151*, 13–28.

(2) Lee, A.; Elam, J. W.; Darling, S. B. Membrane Materials for Water Purification: Design, Development, and Application. *Environ. Sci. Water Res. Technol.* **2016**, *2*, 17–42.

(3) Dudchenko, A. V.; Rolf, J.; Shi, L.; Olivas, L.; Duan, W.; Jassby, D. Coupling Underwater Superoleophobic Membranes with Magnetic Pickering Emulsions for Fouling-Free Separation of Crude Oil/Water Mixtures: An Experimental and Theoretical Study. *ACS Nano* **2015**, *9*, 9930–9941.

(4) Gao, S.; Sun, J.; Liu, P.; Zhang, F.; Zhang, W.; Yuan, S.; Li, J.; Jin, J. A Robust Polyionized Hydrogel with an Unprecedented Underwater Anti-Crude-Oil-Adhesion Property. *Adv. Mater.* **2016**, *28*, 5307–5314.

(5) Xue, Z.; Wang, S.; Lin, L.; Chen, L.; Liu, M.; Feng, L.; Jiang, L. A Novel Superhydrophilic and Underwater Superoleophobic Hydrogel-Coated Mesh for Oil/Water Separation. *Adv. Mater.* **2011**, *23*, 4270–4273.

(6) Zhang, W.; Shi, Z.; Zhang, F.; Liu, X.; Jin, J.; Jiang, L. Superhydrophobic and Superoleophilic PVDF Membranes for Effective Separation of Water-in-Oil Emulsions with High Flux. *Adv. Mater.* **2013**, *25*, 2071–2076.

(7) Kota, A. K.; Kwon, G.; Choi, W.; Mabry, J. M.; Tuteja, A. Hygro-Responsive Membranes for Effective Oilg-Water Separation. *Nat. Commun.* **2012**, *3*, 1025.

(8) Tao, M.; Xue, L.; Liu, F.; Jiang, L. An Intelligent Superwetting PVDF Membrane Showing Switchable Transport Performance for Oil/Water Separation. *Adv. Mater.* **2014**, *26*, 2943–2948.

(9) Zhang, W.; Zhu, Y.; Liu, X.; Wang, D.; Li, J.; Jiang, L.; Jin, J. Salt-Induced Fabrication of Superhydrophilic and Underwater Superoleophobic PAA-g-PVDF Membranes for Effective Separation of Oil-in-Water Emulsions. *Angew. Chemie - Int. Ed.* **2014**, *53*, 856–860.

(10) Huang, S.; Wang, D. A Simple Nanocellulose Coating for Self-Cleaning upon Water Action: Molecular Design of Stable Surface Hydrophilicity. *Angew. Chemie - Int. Ed.* **2017**, *56*, 9053–9057.

(11) Chen, P. C.; Xu, Z. K. Mineral-Coated Polymer Membranes with Superhydrophilicity and Underwater Superoleophobicity for Effective Oil/Water Separation. *Sci. Rep.* **2013**, *3*, 2776.

(12) He, K.; Duan, H.; Chen, G. Y.; Liu, X.; Yang, W.; Wang, D. Cleaning of Oil Fouling with Water Enabled by Zwitterionic Polyelectrolyte Coatings: Overcoming the Imperative Challenge of Oil-Water Separation Membranes. *ACS Nano* **2015**, *9*, 9188–9198.

(13) Liu, X.; Zhou, J.; Xue, Z.; Gao, J.; Meng, J.; Wang, S.; Jiang, L. Clam's Shell Inspired High-Energy Inorganic Coatings with Underwater Low Adhesive Superoleophobicity. *Adv. Mater.* **2012**, *24*, 3401–3405.

(14) Guo, T.; Heng, L.; Wang, M.; Wang, J.; Jiang, L. Robust Underwater Oil-Repellent Material Inspired by Columnar Nacre. *Adv. Mater.* **2016**, 8505–8510.

(15) Zhang, F.; Zhang, W. Bin; Shi, Z.; Wang, D.; Jin, J.; Jiang, L. Nanowire-Haired Inorganic Membranes with Superhydrophilicity and Underwater Ultralow Adhesive Superoleophobicity for High-Efficiency Oil/Water Separation. *Adv. Mater.* **2013**, *25*, 4192–4198.

(16) Zhang, S.; Jiang, G.; Gao, S.; Jin, H.; Zhu, Y.; Zhang, F.; Jin, J. J. Cupric Phosphate Nanosheets-Wrapped Inorganic Membranes with Superhydrophilic and Outstanding Anti-Crude-Oil Fouling Property for Oil / Water Separation. **2018**, *12*, 795-803.

(17) Wen, Q.; Di, J.; Jiang, L.; Yu, J.; Xu, R. Zeolite-Coated Mesh Film for Efficient Oil-Water Separation. *Chem. Sci.* **2013**, *4*, 591–595.

(18) Fakhru'l-Razi, A.; Pendashteh, A.; Abdullah, L. C.; Biak, D. R. A.; Madaeni, S. S.; Abidin, Z. Z. Review of Technologies for Oil and Gas Produced Water Treatment. *J. Hazard. Mater.* **2009**, *170*, 530–551.

(19) Chen, P.-C.; Wan, L.-S.; Xu, Z.-K. Bio-Inspired $CaCO_3$ Coating for Superhydrophilic Hybrid Membranes with High Water Permeability. *J. Mater. Chem.* **2012**, *22*, 22727.

(20) Yang, H. C.; Pi, J. K.; Liao, K. J.; Huang, H.; Wu, Q. Y.; Huang, X. J.; Xu, Z. K. Silica-Decorated Polypropylene Microfiltration Membranes with a Mussel-Inspired Intermediate Layer for Oil-in-Water Emulsion Separation. *ACS Appl. Mater. Interfaces* **2014**, *6*, 12566–12572.

(21) Yang, H.-C.; Chen, Y.-F.; Ye, C.; Jin, Y.-N.; Li, H.; Xu, Z.-K. Polymer Membrane with a Mineral Coating for Enhanced Curling Resistance and Surface Wettability. *Chem. Commun.* **2015**, *51*, 12779–12782.

(22) Wang, Q.; Wang, X.; Wang, Z.; Huang, J.; Wang, Y. PVDF Membranes with Simultaneously Enhanced Permeability and Selectivity by Breaking the Tradeoff Effect *via* Atomic Layer Deposition of TiO_2. *J. Memb. Sci.* **2013**, *442*, 57–64.

(23) Hyde, G. K.; Scarel, G.; Spagnola, J. C.; Peng, Q.; Lee, K.; Gong, B.; Roberts, K. G.; Roth, K. M.; Hanson, C. A.; Devine, C. K.; Stewart, S. M.; Hojo, D.; Na, J.-S.; Jur, J. S.; Parsons, G. N. Atomic Layer Deposition and Abrupt Wetting Transitions on Nonwoven Polypropylene and Woven Cotton Fabrics. *Langmuir* **2010**, *26*, 2550–2558.

(24) Dameron, A.; Davidson, S.; Burton, B.; Carcia, P.; McLean, R.; George, S. Gas Diffusion Barriers on Polymers Using Multilayers Fabricated by Al_2O_3 and Rapid SiO_2 Atomic Layer Deposition. *J. Phys. Chem. C* **2008**, *112*, 4573–4580.

(25) Gebhard, M.; Mai, L.; Banko, L.; Mitschker, F.; Hoppe, C.; Jaritz, M.; Kirchheim, D.; Zekorn, C.; De Los Arcos, T.; Grochla, D.; Dahlmann R.; Grundmeier, G.; Awakowicz, P.; Ludwig, A.; Devi, A. PEALD of SiO_2 and Al_2O_3 Thin Films on Polypropylene: Investigations of the Film Growth at the Interface, Stress, and Gas Barrier Properties of Dyads. *ACS Appl. Mater. Interfaces* **2018**, *10*, 7422–7434.

(26) Lee, S. M.; Pippel, E.; Moutanabbir, O.; Gunkel, I.; Thurn-Albrecht, T.; Knez, M. Improved Mechanical Stability of Dried Collagen Membrane after Metal Infiltration. *ACS Appl. Mater. Interfaces* **2010**, *2*, 2436–2441.

(27) Chen, H.; Lin, Q.; Xu, Q.; Yang, Y.; Shao, Z.; Wang, Y. Plasma Activation and Atomic Layer Deposition of TiO_2 on Polypropylene Membranes for Improved Performances of Lithium-Ion Batteries. *J. Memb. Sci.* **2014**, *458*, 217–224.

(28) Xiong, S.; Yang, Y.; Zhong, Z.; Wang, Y. One-Step Synthesis of Carbon-Hybridized ZnO on Polymeric Foams by Atomic Layer Deposition for Efficient Absorption of Oils from Water. *Ind. Eng. Chem. Res.* **2018**, *57*, 1269–1276.

(29) Xiong, S.; Kong, L.; Huang, J.; Chen, X.; Wang, Y. Atomic-Layer-Deposition-Enabled Nonwoven Membranes with Hierarchical ZnO Nanostructures for Switchable Water/Oil Separations. *J. Memb. Sci.* **2015**, *493*, 478–485.

(30) Barry, E.; Libera, J. A.; Mane, A. U.; Avila, J. R.; DeVitis, D.; Dyke, K. Van; Elam, J. W.; Darling, S. B. Mitigating Oil Spills in the Water Column. *Environ. Sci. Water Res. Technol.* **2018**, *4*, 40–47.

(31) Barry, E.; Mane, A. U.; Libera, J. A.; Elam, J. W.; Darling, S. B. Advanced Oil Sorbents Using Sequential Infiltration Synthesis. *J. Mater. Chem. A* **2017**, *5*, 2929–2935.

(32) Steele, A.; Bayer, I.; Loth, E. Inherently Superoleophobic Nanocomposite Coatings by Spray Atomization. *Nano Lett.* **2009**, *9*, 501–505.

(33) Kota, A. K.; Kwon, G.; Tuteja, A. The Design and Applications of Superomniphobic Surfaces. *NPG Asia Mater.* **2014**, *6*, e109-16.

(34) Clint, J. H.; Wicks, A. C. Adhesion under Water: Surface Energy Considerations. *Int. J. Adhes. Adhes.* **2001**, *21*, 267–273.

(35) Bandura, A. V.; Sofo, J. O.; Kubicki, J. D. Derivation of Force Field Parameters for SnO2-H2O Surface Systems from Plane-Wave Density Functional Theory Calculations. *J. Phys. Chem. B* **2006**, *110*, 8386–8397.

(36) Adiga, S. P.; Zapol, P.; Curtiss, L. A. Structure and Morphology of Hydroxylated Amorphous Alumina Surfaces. *J. Phys. Chem. C* **2007**, *111*, 7422–7429.

(37) Bandura, A. V.; Kubicki, J. D. Derivation of Force Field Parameters for TiO_2−H_2O Systems from Ab Initio Calculations. *J. Phys. Chem. B* **2003**, *107*, 11072–11081.
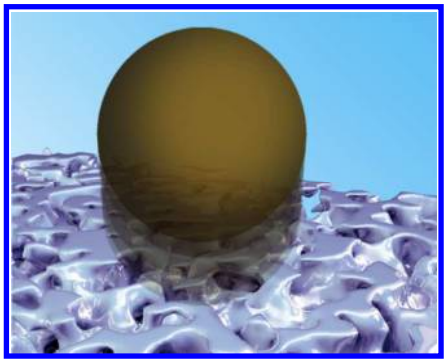
TOC graphic